Received: 23 January 2022 | Revised: 7 March 2022 | Accepted: 23 March 2022

DOI: 10.1002/jcc.26861

SOFTWARE NOTE

Journal of COMPUTATIONAL CHEMISTRY WILEY

Overreact, an in silico lab: Automative quantum chemical microkinetic simulations for complex chemical reactions

Felipe S. S. Schneider | Giovanni F. Caramori

Department of Chemistry, Federal University of Santa Catarina, Florianópolis, Santa Catarina, Brazil

Correspondence
Giovanni F. Caramori, Department of Chemistry, Federal University of Santa Catarina, Florianópolis, SC 88040-900, Brazil.
Email: giovanni.caramori@ufsc.br

Funding information
National Council for Scientific and Technological Development, Grant/Award Numbers: 140485/2017-1, 311132/2020-0

Abstract

Today's demand for precisely predicting chemical reactions from first principles requires research to go beyond Gibbs' free energy diagrams and consider other effects such as concentrations and quantum tunneling. The present work introduces overreact, a novel Python package for propagating chemical reactions over time using data from computational chemistry only. The overreact code infers all differential equations and parameters from a simple input that consists of a set of chemical equations and quantum chemistry package outputs for each chemical species. We evaluate some applications from the literature: gas-phase eclipsed-staggered isomerization of ethane, gas-phase umbrella inversion of ammonia, gas-phase degradation of methane by chlorine radical, and three solvation-phase reactions. Furthermore, we comment on a simple solvation-phase acid–base equilibrium. We show how it is possible to achieve reaction profiles and information matching experiments.

KEYWORDS
chemical reactions, concentration effects, in silico experiments, microkinetic modeling, overreact, Python3

1 | INTRODUCTION

Many of the challenges of this century, such as producing fuels and chemicals from biomass[1–4] and greenhouse gases,[5–8] as well as developing greener synthetic protocols,[9–12] encompass problems related with both chemical kinetics and catalysis. Improving the understanding of reaction mechanisms is mandatory to meet the demand in designing efficient catalysts and molecular machines of increasingly complex behavior, needed to overcome such challenges in a sustainable and efficient manner.[4,13–15]

The demand for rational design of reactions, catalysts, and chemical devices is leading our community towards the development of accurate and efficient computational modeling tools and methodologies.[13,16–18] Despite the challenges in predicting observed reaction rate constants correctly, by using first principle calculations, the recent growth[19] of computing resources and methodological developments have made the calculation of complex reaction mechanisms almost routine.[16,18,20–26] This has uniquely aided both the elucidation of experiments and the comprehension of complex chemical phenomena.[13,16]

Notwithstanding, feasible mechanistic propositions must be calculated with adequate levels of theory[27] and take into account all the relevant physics of the problem. The computational modeling of chemical reactions is a complex topic due to the overwhelming set of physical considerations that are required,[28] and the quest for mechanistic understandings actually requires a significant amount of automation,[16,18] being therefore necessary to consider effects such as pre-equilibrium and concentration,[23] dispersion corrections,[29,30] solvation,[30–32] molecular symmetry,[30] proper treatment of Gibbs energy contributions,[29,30,32,33] standard state corrections,[30–32] tunneling and others.[28,30]

Even so, most of the modeling of chemical reactions based on first-principles calculations is done using reaction rate constants alone, which is oftentimes not enough. Comparison with the experiment requires reaction rates, which depend on concentrations. For instance, the outcome and selectivity of two competing second-order reactions such as $R + A \rightarrow \mathbf{P}_A$ and $R + B \rightarrow \mathbf{P}_B$, whose kinetic equations are given by $d[\mathbf{P}_A]/dt = \mathbf{k}_1$ [R][A] and $d[\mathbf{P}_B]/dt = \mathbf{k}_2$ [R][B], are undoubtedly dependent not only on the rate constants k_1 and k_2, but also on the concentrations [A] and [B].[23] Furthermore, it is well known that a

TABLE 1 Comparison of programs in the literature for theoretical chemical kinetics. Partially adapted from Dzib et al.[38] (only available software indicated).

Program	Theory	Molecularity	Phase	Tunnel effect	Language
overreact	TST	Any	Gas, solution	Wigner, Eckart	Python
Eyringpy	TST, MT, CKT	Uni/bi	Gas, solution	Wigner, Eckart	Python
Polyrate	TST, VTST, RRKM	Uni/bi	Gas, solid, gas–solid	ZCT, SCT, LCT	Fortran
MultiWell	ME, RRKM	Uni	Gas	–	Fortran
TAMkin	TST	Uni/bi	Gas	Wigner, Eckart	Python
MESMER	ME, RRKM	Uni/bi	Gas, solution	Eckart	C++
KiSThelp	TST, VTST, RRKM	Uni/bi	Gas	Wigner, Eckart	Java
RMG	TST, CKT	Uni/bi	Gas, solution	Wigner, Eckart	Python
APUAMA	TST	Uni/bi	Gas	Wigner, Eckart, SCT	C++
Pilgrim[59]	TST, VTST, CVT	Uni/bi	Gas	SCT	Python

Abbreviations: CKT, Collins–Kimbal Theory; CVT, canonical variational transition state theory; LCT, large curvature tunneling; ME, master equation; MT, Marcus theory; RRKM, Rise–Ramsperger–Kassel–Marcus; SCT, small curvature tunneling; VTST, variational transition state theory; ZCT, zero curvature tunneling.

single reaction step may not be enough to determine a whole chemical reaction path or catalytic cycle,[34–36] bringing ambiguity in the general concept of "rate-determining step."[35] The reasoning becomes still more entangled when a single observed reaction rate law is taken into consideration, such as when two steps with similar barriers within a single mechanism exist or when concurrent mechanisms coexist with an equal probability of occurring. Those problems have led to the development of new analytical tools, broadening the interpretation of reactions and, in particular, catalytic processes.[34,36,37]

A useful solution to these issues is to simulate reaction models whose parameters are taken from computational chemistry calculations. For instance, modeling reactions using microkinetic simulations has become increasingly important, especially when it is essential to take concentration effects into account.[23] First-principle calculations have allowed us to calculate binding free energies[30] and reaction rate constants[38] reasonably close to experimental values, as long as the correct physical phenomena are appropriately addressed. This idea is not new in the experimental laboratory: Blackmond have advocated using full-blown kinetics simulations to elucidate experimentally observed reaction mechanisms through model exploration.[34,36] This analysis protocol has been shown to be crucial for elucidating many mechanisms of industrial importance. Similarly, microkinetic models provide time-resolved kinetic analysis that allows one to consolidate, analyze and test hypotheses in catalysis and chemical kinetics in general,[34,36] and it has extensively used in computational heterogeneous catalysis,[15,39–55] experimental biology[56] and mechanism validation.[57] It is thus possible to accurately perform first-principles microkinetic simulations on rather complex reaction phenomena over time, which allows one to better comprehend tricky aspects not revealed by more simplistic models.[34,36] Even with possible systematic errors brought by first-principle calculations, insights are warranted.[35,37,58]

Unfortunately, there is currently no general solution for first-principles microkinetic modeling that, simultaneously, (1) calculates all the required thermochemical quantities and corrections from first-principles, (2) automatically calculates reaction rate constants, including quantum tunneling approximations, for all reactions, (3) generates an (usually non-linear) ordinary differential equation (ODE) system from an arbitrary reaction scheme automatically, (4) produces a Jacobian for the ODE system using automatic differentiation for improved accuracy and performance, and (5) propagates the chemical kinetic processes generating concentrations for all compounds as a function of time and initial concentrations. Table 1 compares the capabilities of overreact with some other known microkinetic software in the literature.

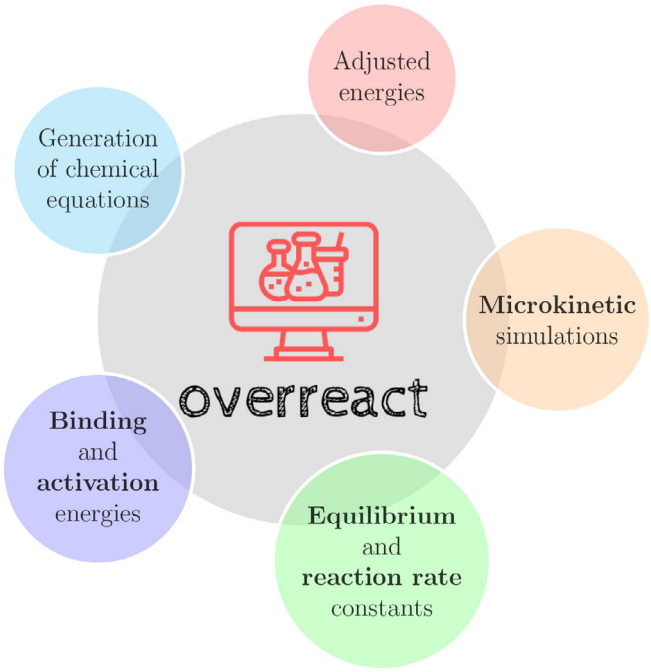

FIGURE 1 Visual depiction of some of the capabilities of overreact, a Python library and command-line tool for building and analyzing homogeneous microkinetic models from first-principles calculations. Instructions on how to install and use can be found at https://geem-lab.github.io/overreact-guide

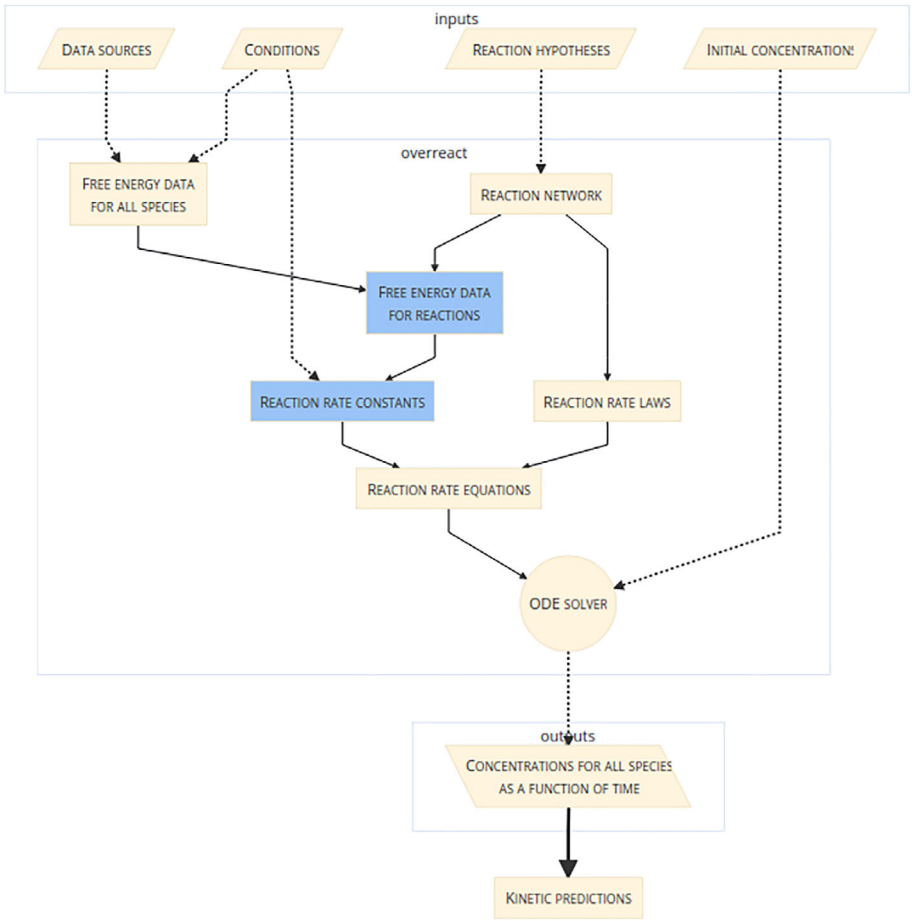

FIGURE 2 A simplified diagram featuring the overreact dataflow. Computational chemistry logfiles are taken as data sources. Together with temperature conditions, a chemical reaction network and initial concentrations, overreact calculates Gibbs' free energies for all species. From this information, reaction rate constants and a system of ordinary differential equations (ODEs) are devised. This ODE system is solved, yielding concentrations for all species over time. Further details can be found in the supporting information

The present work presents a simple yet robust software that treats all the five points listed above in an automated way, starting from the outputs of ab initio calculations of numerous levels of theory (Density Functional Theory, Hartree-Fock, post-Hartree-Fock or any other where Hessian calculations are available).[60] It is able to solve any chemical reaction network, including parallel and concurrent reactions, from elementary steps at constant temperature in the well-stirred approximation. The key features of the proposed code, called overreact, are highlighted in Figure 1. It has been have developed as a user-friendly, open-source (MIT license) Python program and library that does simple and automatic microkinetic modeling of complex reaction networks in solution and gas-phase using only the user description of the reactions to be considered in the model, the corresponding computational chemistry output files, initial concentrations, and a set of reaction conditions such as temperature. Only the converged geometries, electronic energies, and vibrational frequencies of each species in the model are required from the outputs. Overreact is freely available, simple to install and use, well tested, well documented, and encompasses an easy-to-use command-line application (https://geem-lab.github.io/overreact-guide/). Although only thoroughly tested with ORCA[61] and Gaussian 09[62] output files at the moment, it employs the Python library cclib[63] for parsing computational chemistry outputs, which is actually known to work with 14 different computational chemistry packages. Overreact not only generates and solves arbitrary chemical kinetic ODE problems, but also allows the user to fix the concentration of one or more compounds, which is useful for simulating reactions in neat or buffered conditions. Furthermore, the user can adjust systematic first-principle absolute Gibbs energy errors by comparison with experiments automatically, which are expected to be up to 4 kcal mol^{-1} even when suitable density functional are employed.[26,64–67]

2 | METHODOLOGY

The overreact code attempts to make the process of building precise chemical microkinetic models from first principle calculations as automatic as possible. It takes data from computational chemistry logfiles and uses them to calculate thermodynamic and kinetic properties, as shown in the dataflow diagram in Figure 2. This information gives rise to reaction rate constants and a system of ordinary differential equations, which, together with initial concentrations, yields concentrations of all species over time.

The dataflow diagram of Figure 2 is simplification of the whole process, not a complete description of the system. A detailed description of the library's core functionalities can be found in the Supporting Information, where automated procedures, methodologies and capabilities implemented in overreact are highlighted.

3 | RESULTS AND DISCUSSION

Representative results of overreact usage are available in the following subsections. Defaults are used when not otherwise specified.

3.1 | Examples in the gas phase

3.1.1 | Simple gas-phase autoisomerizations

In order to demonstrate that overreact can estimate precise reaction rate constants from ab initio calculations, we first consider some simple gas-phase autoisomerization reactions.

Ethane

We estimated the rate of autoisomerization of the ethane from staggered to eclipsed back to staggered again. At B97-3c,[68] the rate calculated was found to be 8.2×10^{10} s^{-1} (including tunneling coefficient of 1.11). Higher levels of theory gave similar results (4.8×10^{10} and 6.3×10^{10} s^{-1}, including tunneling coefficients of 1.13 and 1.12, for 6-311G(d,p) and UMP2/6-311G(3df,3pd), respectively). There is overall good agreement with the experimental estimate of 8.3×10^{10} s^{-1}.[69]

Ammonia

The reaction rate constant for the umbrella inversion of ammonia was estimated to be 1.3×10^{10} s^{-1} at MP2/ma-def2-TZVP (tunneling coefficient $\kappa = 2.00$), which agrees with the experimental value of 4×10^{10} s^{-1}.[70] On the other hand, the barrier at MP2/ma-def2-TZVP was found to be 4.1 kcal mol^{-1}, lower than the experimental one (5.8 kcal mol^{-1}).[70] A calculation at CCSD(T)/cc-pVTZ better agrees with the thermodynamical barrier (6.0 kcal mol^{-1}), but degrades the reaction rate constant (5.9×10^{8} s^{-1}, with $\kappa = 2.37$). Similar results were found using DFT ($\Delta G^{\ddagger} = 5.4$ kcal mol^{-1} and $k = 3.6 \times 10^{9}$ s^{-1} with $\kappa = 4.88$ at ωB97X-D4-gCP/def2-TZVP), suggesting that the Eckart approximation is not enough to get quantitative results in this particular case, as one of the key assumptions of the model is that the reaction takes place through a linear path in the potential energy surface.

3.1.2 | $CH_4 + Cl \rightarrow CH_3 + HCl$

Tanaka et al. studied the degradation of methane by chlorine radical gas in the context of the global methane cycle in the atmosphere.[71] In line with the results reported by Dzib et al.,[38] we obtained a reaction rate constant of 9.3×10^{-14} cm^3 $molecule^{-1}$ s^{-1} ($\kappa = 3.64$) at UMP2/cc-pVTZ for this bimolecular reaction, in line with previous computational results of Tanaka et al.[71] (2.2×10^{-13} cm^3 $molecule^{-1}$ s^{-1}) and the current recommended experimental value of 1.0×10^{-13} cm^3 $molecule^{-1}$ s^{-1}.[72] Overall, the calculated reaction rate constants using the Eckart tunneling approximation fall in the lower range of the experimental 95% confidence interval in the range 181–300 K (Figure 3A), in excellent agreement with experimental results in that range ($r^2 = 0.9984$, Figure 3B). Furthermore, a one-second microkinetic modeling of this fast gas-phase reaction example (using as initial concentrations 250, 100, and 25 nM for CH_4, Cl., and HCl, respectively) is shown in Figure 3c, where the concentrations of all species are obtained as a function of time.

3.2 | Examples in solution

3.2.1 | Constrained equilibria: acetic acid-acetate equilibrium concentrations versus pH

overreact is able to calculate simple equilibrium systems without knowledge of reaction rate constants by producing them such that equilibrium constants are satisfied. When used together in a reaction network, the algorithm ensures that the fictitious, calculated forward and backwards reaction rate constants are larger than any other reaction rate constant in the system by a factor of eight. Although it makes equations stiffer, this allows investigating systems containing both equilibria and fast reactions together, as is indicated in the following sections.

On the other hand, pure equilibria can still be useful. Even though it is not possible to obtain *quantitative* kinetic profiles with equilibria alone, it is perfectly reasonable to obtain final Boltzmann populations from them. In fact, together with a simple constraint optimizer implemented in overreact, it is possible to fix the concentrations of any part of the system and check how this would affect the final populations.

In order to assess the correctness of pure equilibria calculations in overreact, as well as the concentration constraining feature, we estimated the final concentrations in solution of the acetic acid-acetate, acid–base equilibrium system. For that, we employed a combination of ab initio calculations and experimental pK_a values to account for systematic errors.[31,73] Different values of pH where fixed by constraining the H^+ concentration.

Optimizations and frequencies for the AcOH(aq) ⇋ AcO^-(aq) + H^+(aq) system were performed at UM06-2X/6-311++G(d,p)/SMD (water).[31,74,75] All data for H^+ was inserted directly in the overreact input. For comparison, two distinct energies for the proton solvation energy were separately employed: −265.9 kcal mol^{-1}, as used in the parameterization process of SMD,[31] and −277.2 kcal mol^{-1}, which is the value that correctly predicts the experimental pK_a of 4.756 for this system.[76] The final calculated concentrations as a function of pH for both proton solvation energies can be seen in Figure 4. As can be seen, although errors are very sensitive to the energy values provided, overreact produces the expected result if precise energy values are provided.

3.2.2 | Hickel (1992)

We compared the applicability of overreact for reactions in solvation using the well-known radical reaction $NH_{3(w)} + OH_{(w)} \rightarrow NH_{2(w)} + H_2O_{(w)}$ at M06-2X-D3(0)/6-311++G(d,p)/SMD(water)[31,74,75] (using ORCA 4.2.1[61]). The calculated reaction rate constant can be seen in Figure 5, together with a comparison with experimental and theoretical results available in the literature (exact figures are available in

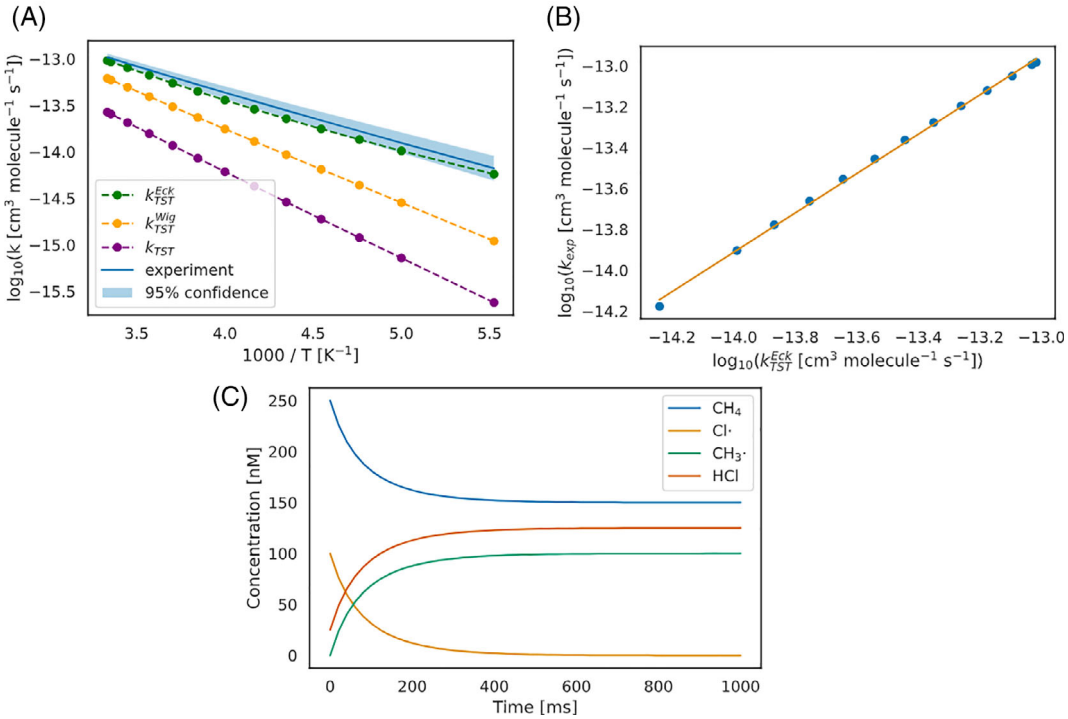

FIGURE 3 Computed chemical kinetics of $CH_4 + Cl \rightarrow CH_3 + HCl$ in the gas phase. (A) Arrhenius plots in the range 181–300 K with different tunneling approximations compared against the recommended experimental fit of Burkholder et al. and its 95% confidence interval.[72] Compare to Figures 1 and 2 of Dzib et al.[38] and Tanaka et al.,[71] respectively. (B) Linear regression between the calculated, Eckart-corrected reaction rate constants against the experimental results, in logarithmic scale ($\log_{10}\left(k_{TST}^{Eck}\right) = 0.9633 \times \log_{10}(k_{exp}) + 0.4256$, $r^2 = 0.9984$). (C) Microkinetic simulation of the gas-phase reaction $CH_4 + Cl \rightarrow CH_3 + HCl$ (using 250, 100, and 25 nM as initial concentrations of CH_4, Cl., and HCl, respectively)

FIGURE 4 Computed acid–base equilibrium for AcOH(aq) ⇋ AcO^-(aq) + H^+(aq) at UM06-2X/6-311++G(d,p)/SMD(water)[31,74,75] for a series of pH values

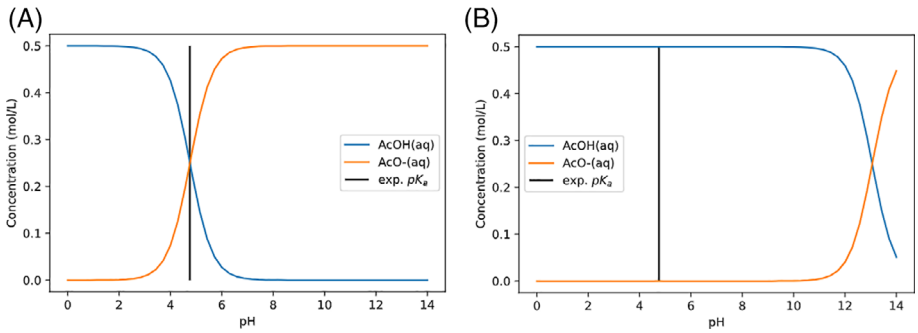

Table S1). The experimental results were all measured at high pH and, since the effect of the ammonia-ammonium equilibrium is negligible in those conditions,[38,77] the phenomenon was not considered in this case for simplicity.

3.2.3 | Pérez-Soto (2020)

Pérez-Soto et al. have applied computer experiments to a well-studied imine formation reaction using techniques very similar to the ones in the present work.[67] Since those reactions encompass a proton transfer, they suffer from effects of residual water, as water can facilitate proton shuttling. Even though the reaction happens in dichloromethane, water is found as an impurity in the commercially-available solvent and, most importantly, it is produced as a by-product in the second, dehydrating step.[67]

Such cases are not uncommon and can hardly be properly rationalized by simple free energy diagrams, requiring microkinetics or other techniques that take into account changes of concentration throughout the reaction.[24,25]

The work of Pérez-Soto et al. is particularly important due to their investigation on systematic errors in bimolecular reaction barriers.[67] This takes place due to the impossibility, for bimolecular reactions, of the common error cancellation found in monomolecular reactions. They not only showed the systematicity of such errors, but also that they could be reduced, for a given reaction, by properly adjusting all Gibbs' free energies with a single tunable parameter.[67]

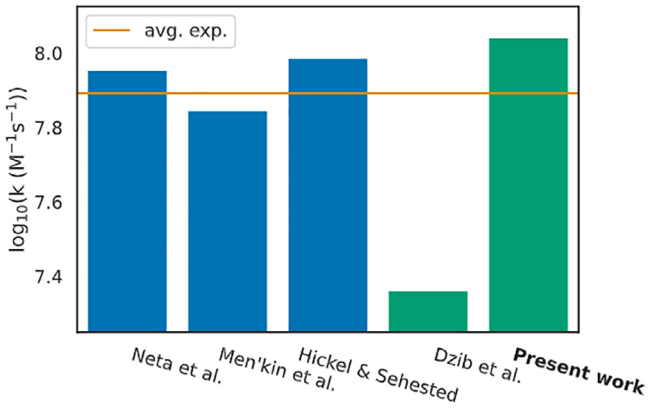

FIGURE 5 Comparison of experimental and computational results from the literature for the reaction rate constant of the reaction $NH_{3(w)} + OH_{(w)} \rightarrow NH_{2(w)} + H_2O_{(w)}$ at M06-2X-D3(0)/6-311++G(d,p)/SMD (water)[31,74,75] (using ORCA 4.2.1[61]). All values indicated are in logarithmic scale. Blue and green bars represent experimental and computational results, respectively. The orange line is the $\log_{10}$ value of the average of experimental values. The exact values can be found in Table S1

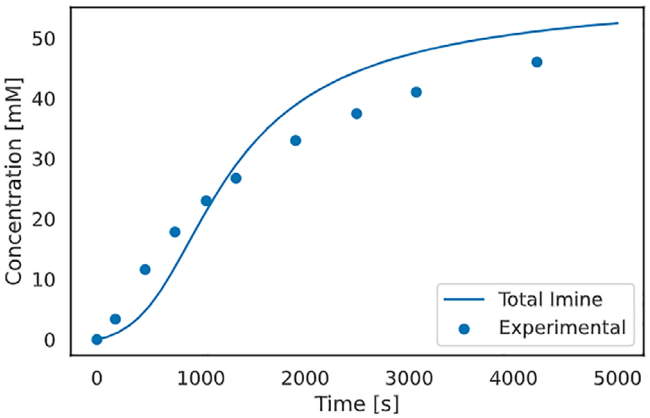

FIGURE 6 Predicted kinetic profile for the reaction of Pérez-Soto et al.[67] experimental data taken from the supporting information of Pérez-Soto et al.[67] is also shown. A systematic bias of 3.2 kcal mol^{-1} was employed in agreement with the original work,[67] which translates to a root-mean-squared deviation (RMSD) of 4.97 mM. The summed concentration of the imine product is shown, as it is found in association with different amine and water quantities. A detailed profile with all relevant species can be found in Figure S3

In Figure 6 a reproduction of their work is shown and compared against experimental concentration data points. The exact same Gibb's free energy adjustment of 3.2 kcal mol^{-1} as employed in the original work was used by us, which is equivalent to a root-mean-squared error of 4.97 mM when compared against the experimental data points. Apart from that, the present results differ from Pérez-Soto et al. in that we employed all additional approximations implemented in overreact: Eckart tunneling corrections for all reaction steps and the quasi-rigid rotor-harmonic approximation for both enthalpies and entropies. The fact that a systematic energy correction was still required to attain experimental-grade quality suggests yet another source of error.

A systematic study on the effect of the tunable parameter can be seen in Figure S2, which shows a flat region around 2–3 kcal mol^{-1}. This suggests that, even though such energy adjustments might be seen as arbitrary, they may make little influence on the final result as long as the chosen value is reasonable. Due to DFT errors in general, fitting systematic deviations in first-principles reaction schemes seems to be warranted and, in the future, this could be performed automatically using available experimental data. Progress is currently being made in this respect in our laboratory.

3.2.4 | Intramolecular amide hydrolysis of N-alkyl maleamic acids

We have looked into intramolecular amide hydrolysis initially investigated by Kirby and Lancaster[78] and subsequently studied by others.[79–81] We employed calculations using ωB97XD/6-311++G**/SMD(water)[31,74,82] and used Gaussian 09 (Revision C.01).[62] As before, the proton energy was adjusted in order to reproduce the experimental pK_a of 4.756 for acetic acid.[76] Three distinct mechanisms proposed in the literature can be seen in Figure 7. One thing that is worth of note in Figure 7 is the step going through $I^{‡}$, which presents a proton transfer in a four-membered ring transition state. While its bare barrier is around 28.8 kcal mol^{-1}, this can be reduced to 13.6 kcal mol^{-1} by the use of a single-water-molecule proton shuttle. Furthermore, while the facilitated transfer shows only an 8% reaction rate constant increase due to tunneling (using the Eckart approximation), the bare reaction step shows a 960 times (!) increase, even at room temperature. Notwithstanding, the product M is not formed during simulation if the facilitated $I^{‡}$ step is removed from the system. All this, together with the indication that the tetrahedral intermediate J appears to be an important rest state, strongly suggests that the step passing through $I^{‡}$ is the rate-determining one, and that it includes active participation of the solvent.

One key feature of this reaction is its strong dependency on pH: as early shown by Kirby and Lancaster, the reaction takes place on acidity environments only.[78] In order to access its behavior in different acidic environments, we employed a series of short (0.5 s) simulations at different pH values, always starting with 0.1 M of the maleamic acid A (Figure 8A). We kept the concentration of H^+ at a different value for each simulation (corresponding to pH 0–7), but we employed pseudo-first order conditions with respect to the solvent in each of them, constraining the water concentration to stay at 55.6 M. In total, the presented system encompasses 25 simultaneous and automatically simulated reactions and 17 distinct species. As can be seen in Figure 8A, the results corroborate with initial velocity essays worked by Kirby and Lancaster for closely-related systems,[78] where reaction ceases to happen around pH 5.

By simulating the whole system for an hour at pH 2, we could obtain the kinetic profile in Figure 8B. Observing the concentration over time of different intermediates leads us to conclude that, under

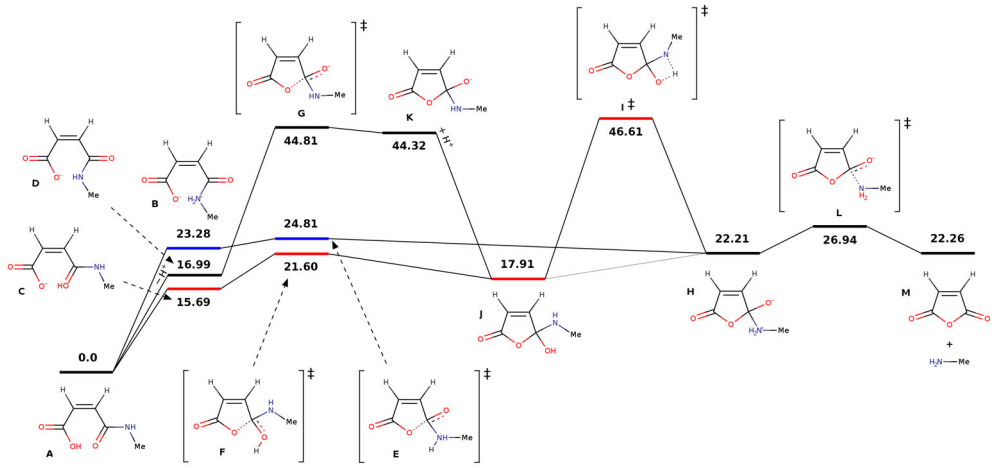

FIGURE 7 Proposed reaction mechanisms for the amide hydrolysis of N-alkyl maleamic acids, as previously proposed in the literature.[78–81] Three possible mechanisms are indicated with distinct colors. The black bars denote the path starting with proton dissociation, followed by an intramolecular attack on the amide carbon. The red bars indicate a path where the attack happens concomitant to a proton transfer to the amide carbonyl. In addition, the blue bars indicate a similar path, but the proton is transferred to the amide nitrogen upon attack on the carbon. Subsequent dissociation of the product complex is worth $\Delta G^{\circ} = -4.74$ kcal mol^{-1}. In the current work, we investigate the base case where $R_1 = -CH_3$ and $R_2 = R_3 = H$

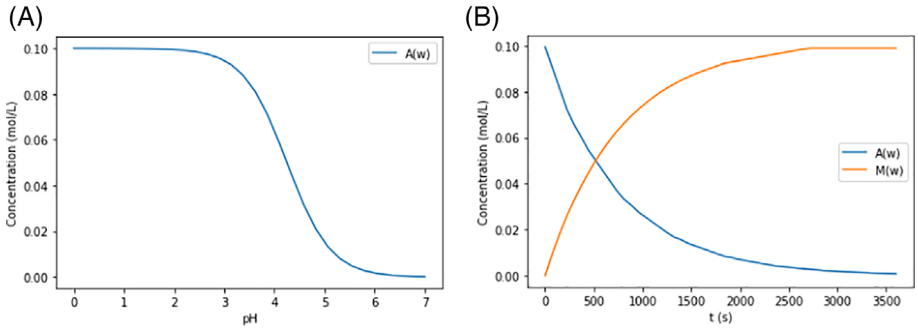

FIGURE 8 (A) Short (0.5 s) simulations at different pH values (pH 0–7). (B) Kinetic profile for the reaction at pH 2, as simulated for an hour (3600 s). In all cases, pseudo-first order conditions with respect to water were maintained (55.6 M) and the initial concentration of the maleamic acid A (Figure 7) was 0.1 M. All reactions presented so far were included in the simulations (25 in total, see text and Figure 7)

these conditions, the reaction seems to happen mostly through equilibrium-state C and rest-state J: as J starts to build up, it gradually transitions, with the help of the solvent, to H, whose C–N bond has been elongated at this point. Finally, after the production of both M and the primary amine leaving group, actual separation further steers the reaction forward due to entropy ($\Delta S^{\circ} = 27$ cal mol^{-1} K^{-1}).

4 | SUMMARY AND OUTLOOK

We applied an automatic process for obtaining reaction kinetic profiles of increasingly complex reactions from first principles. The presented method allows for direct comparison with experimentally obtained results, which are often indispensable when studying chemical reactions.[16] Known disparities can be systematically adjusted using energetic biases if the computational model is known to deliver systematic errors, which is particularly important in systems involving bimolecular reactions.

Although not a magic blackbox, overreact offers a hopefully complete but simple predictive computational environment for hypothesis testing in first-principles homogeneous chemical kinetics and catalysis. In fact, from the calculated concentrated curves using microkinetic simulations, observed reaction rate constants can be inferred using the same mathematical techniques employed in common experimental data treatments.[34,36]

The open-source package presented in this article is already available to explore and analyze reaction mechanisms. Detailed instructions on how to install and use can be found at https://geem-lab.github.io/overreact-guide/. In the future, we will investigate the applicability of overreact to more complex, catalytic systems,[83,84] extend the present work to heterogeneous reactions, and attempt to fully predict the outcome of reactors by coupling computational fluid dynamics with first-principles microkinetic modeling.[85] All this would, in principle, allow us to design catalysts that work well in the scale they are meant to.

ACKNOWLEDGMENTS

The authors Felipe S. S. Schneider and Giovanni F. Caramori thank the National Council for Scientific and Technological Development, CNPq for their PhD (140485/2017-1) and research (311132/2020-0) grants, respectively.

DATA AVAILABILITY STATEMENT

Data that supports the findings of this study are available in the supplementary material of this article. A complete data set is openly available in https://github.com/geem-lab/overreact-data. The source code of overreact is also openly available at https://github.com/geem-lab/overreact. A user guide can be found at https://geem-lab.github.io/overreact-guide/.

ORCID

Felipe S. S. Schneider https://orcid.org/0000-0001-8090-2976
Giovanni F. Caramori https://orcid.org/0000-0002-6455-7831

REFERENCES

[1] D. Klass, *Biomass for Renewable Energy, Fuels, and Chemicals*, Academic Press, Cambridge, Massachusetts **1998**.
[2] A. Demirbaş, *Energy Convers. Manag.* **2001**, *42*, 1357.
[3] J. B. Binder, R. T. Raines, *J. Am. Chem. Soc.* **2009**, *131*, 1979.
[4] R. Šivec, M. Grilc, M. Huš, B. Likozar, *Ind. Eng. Chem. Res.* **2019**, *58*, 16018.
[5] M. Auffhammer, V. Ramanathan, J. R. Vincent, *Proc. Natl. Acad. Sci.* **2006**, *103*, 19668.
[6] H. V. M. Hamelers, O. Schaetzle, J. M. Paz-García, P. M. Biesheuvel, C. J. N. Buisman, *Environ. Sci. Technol. Lett.* **2013**, *1*, 31.
[7] V. Barbarossa, G. Vanga, R. Viscardi, D. M. Gattia, *Energy Procedia* **2014**, *45*, 1325.
[8] J. Fanchi, C. Fanchi, *Energy IN THe 21st Century*, 4th ed., World Scientific Publishing Company, Hackensack, NJ **2016**.
[9] P. Raveendran, J. Fu, S. L. Wallen, *J. Am. Chem. Soc.* **2003**, *125*, 13940.
[10] A. Arcadi, *Chem. Rev.* **2008**, *108*, 3266.
[11] P. Anastas, N. Eghbali, *Chem. Soc. Rev.* **2010**, *39*, 301.
[12] O. V. Kharissova, B. I. Kharisov, C. M. Oliva González, Y. P. Méndez, I. López, *R. Soc. Open Sci.* **2019**, *6*, 191378.
[13] D. J. Tantillo, C. Jiangang, K. N. Houk, *Curr. Opin. Chem. Biol.* **1998**, *2*, 743.
[14] K. N. Houk, F. Liu, *Acc. Chem. Res.* **2017**, *50*, 539.
[15] Y. Wang, L. Xiao, Y. Qi, M. Mahmoodinia, X. Feng, J. Yang, Y.-A. Zhu, D. Chen, *Phys. Chem. Chem. Phys.* **2019**, *21*, 19269.
[16] S. Ahn, M. Hong, M. Sundararajan, D. H. Ess, M.-H. Baik, *Chem. Rev.* **2019**, *119*, 6509.
[17] J. W. Kim, Y. Kim, K. Y. Baek, K. Lee, W. Y. Kim, *Chem. A Eur. J.* **2019**, *123*, 4796.
[18] I. Funes-Ardoiz, F. Schoenebeck, *Chem* **2020**, *6*, 1904.
[19] M. S. Gordon, G. Barca, S. S. Leang, D. Poole, A. P. Rendell, J. L. Galvez Vallejo, B. Westheimer, *Chem. A Eur. J.* **2020**, *124*, 4557.
[20] N. Nikbin, S. Caratzoulas, D. G. Vlachos, *ChemCatChem* **2012**, *4*, 504.
[21] J. Jover, *Phys. Chem. Chem. Phys.* **2017**, *19*, 29344.
[22] W. Guo, R. Kuniyil, J. E. Gómez, F. Maseras, A. W. Kleij, *J. Am. Chem. Soc.* **2018**, *140*, 3981.
[23] M. Besora, F. Maseras, *Wiley Interdiscip. Rev.: Comput. Mol. Sci.* **2018**, *8*, e1372.
[24] Y. Yu, Y. Zhu, M. N. Bhagat, A. Raghuraman, K. F. Hirsekorn, J. M. Notestein, S. T. Nguyen, L. J. Broadbelt, *ACS Catal.* **2018**, *8*, 11119.
[25] M. Jaraíz, J. E. Rubio, L. Enríquez, R. Pinacho, J. L. López-Pérez, A. Lesarri, *ACS Catal.* **2019**, *9*, 4804.
[26] A. Ishikawa, Y. Tateyama, *J. Comput. Chem.* **2019**, *40*, 1866.
[27] P. Morgante, R. Peverati, *Int. J. Quantum Chem.* **2020**, *120*, e26332.
[28] H. Ryu, J. Park, H. K. Kim, J. Y. Park, S.-T. Kim, M.-H. Baik, *Organometallics* **2018**, *37*, 3228.
[29] S. Grimme, *Chem. Eur. J.* **2012**, *18*, 9955.
[30] J. H. Jensen, *Phys. Chem. Chem. Phys.* **2015**, *17*, 12441.
[31] A. V. Marenich, C. J. Cramer, D. G. Truhlar, *J. Phys. Chem. B* **2009**, *113*, 6378.
[32] R. F. Ribeiro, A. V. Marenich, C. J. Cramer, D. G. Truhlar, *J. Phys. Chem. B* **2011**, *115*, 14556.
[33] Y.-P. Li, J. Gomes, S. Mallikarjun Sharada, A. T. Bell, M. Head-Gordon, *J. Phys. Chem. C* **2015**, *119*, 1840.
[34] D. G. Blackmond, *Angew. Chem. Int. Ed.* **2005**, *44*, 4302.
[35] S. Kozuch, J. M. L. Martin, *ChemPhysChem* **2011**, *12*, 1413.
[36] D. G. Blackmond, *J. Am. Chem. Soc.* **2015**, *137*, 10852.
[37] E. Solel, N. Tarannam, S. Kozuch, *Chem. Commun.* **2019**, *55*, 5306.
[38] E. Dzib, J. L. Cabellos, F. Ortíz-Chi, S. Pan, A. Galano, G. Merino, *Int. J. Quantum Chem.* **2018**, *119*, e25686.
[39] J. A. Dumesic, D. F. Rudd, D. F. Rudd, L. M. Aparicio, J. E. Rekoske, A. A. Trevino, *The microkinetics of heterogeneous catalysis*, American Chemical Society, **1993**.
[40] A. van de Runstraat, J. van Grondelle, R. A. van Santen, *Ind. Eng. Chem. Res.* **1997**, *36*, 3116.
[41] M. Neurock, E. W. Hansen, *Comput. Chem. Eng.* **1998**, *22*, S1045.
[42] A. B. Mhadeshwar, H. Wang, D. G. Vlachos, *J. Phys. Chem. B* **2003**, *107*, 12721.
[43] A. Bhan, S. Hsu, G. Blau, J. Caruthers, V. Venkatasubramanian, W. Delgass, *J. Catal.* **2005**, *235*, 35.
[44] L. C. Grabow, A. A. Gokhale, S. T. Evans, J. A. Dumesic, M. Mavrikakis, *J. Phys. Chem. C* **2008**, *112*, 4608.
[45] G. Novell-Leruth, J. M. Ricart, J. Pérez-Ramírez, *J. Phys. Chem. C* **2008**, *112*, 13554.
[46] S. C. Ammal, A. Heyden, *J. Phys. Chem. Lett.* **2012**, *3*, 2767.
[47] R. A. van Santen, A. J. Markvoort, I. A. W. Filot, M. M. Ghouri, E. J. M. Hensen, *Phys. Chem. Chem. Phys.* **2013**, *15*, 17038.
[48] A. J. Medford, C. Shi, M. J. Hoffmann, A. C. Lausche, S. R. Fitzgibbon, T. Bligaard, J. K. Nørskov, *Catal. Lett.* **2015**, *145*, 794.
[49] C. F. Goldsmith, R. H. West, *J. Phys. Chem. C* **2017**, *121*, 9970.
[50] Y. Mao, H. Wang, P. Hu, *WIREs* **2017**, *7*, e1321.
[51] Z. Chen, H. Wang, N. Q. Su, S. Duan, T. Shen, X. Xu, *ACS Catal.* **2018**, *8*, 5816.
[52] L. Foppa, K. Larmier, A. Comas-Vives, *CHIMIA Int. J. Chem.* **2019**, *73*, 239.
[53] J. Park, J. Cho, Y. Lee, M.-J. Park, W. B. Lee, *Ind. Eng. Chem. Res.* **2019**, *58*, 8663.
[54] H. Liu, J. Liu, B. Yang, *Phys. Chem. Chem. Phys.* **2019**, *21*, 9876.
[55] M. Huš, M. Grilc, A. Pavlišič, B. Likozar, A. Hellman, *Catal. Today* **2019**, *338*, 128.
[56] A. L. Slusarczyk, A. Lin, R. Weiss, *Nat. Rev. Genet.* **2012**, *13*, 406.
[57] M. O. Miranda, Y. DePorre, H. Vazquez-Lima, M. A. Johnson, D. J. Marell, C. J. Cramer, W. B. Tolman, *Inorg. Chem.* **2013**, *52*, 13692.
[58] R. Christensen, H. A. Hansen, T. Vegge, *Cat. Sci. Technol.* **2015**, *5*, 4946.
[59] Ferro-Costas, D.; Truhlar, D. G.; Fernández-Ramos, A. Pilgrim: A thermal rate constant calculator and kinetics Monte Carlo Simulator (version 1.0). https://github.com/daferro/Pilgrim, **2019**; Accessed: March 2022.
[60] Schneider, F. S. S. geem-lab/overreact: v1.0.2. **2021**; https://zenodo.org/record/5730603.
[61] F. Neese, *WIREs Comput. Mol. Sci.* **2017**, *8*, e1327.
[62] M. J. Frisch, G. W. Trucks, H. B. Schlegel, G. E. Scuseria, M. A. Robb, J. R. Cheeseman, G. Scalmani, V. Barone, G. A. Petersson, H. Nakatsuji, X. Li, M. Caricato, A. V. Marenich, J. Bloino, B. G. Janesko, R. Gomperts, B. Mennucci, H. P. Hratchian, J. V. Ortiz, A. F. Izmaylov, J. L. Sonnenberg, D. Williams-Young, F. Ding, F. Lipparini, F. Egidi, J. Goings, B. Peng, A. Petrone, T. Henderson, D. Ranasinghe, V. G. Zakrzewski, J. Gao, N. Rega, G. Zheng, W. Liang, M. Hada, M. Ehara, K. Toyota, R. Fukuda, J. Hasegawa, M. Ishida, T. Nakajima, Y. Honda, O. Kitao, H. Nakai, T. Vreven, K. Throssell, J. A. Montgomery Jr., J. E. Peralta, F. Ogliaro, M. J. Bearpark, J. J. Heyd, E. N. Brothers, K. N. Kudin, V. N. Staroverov, T. A. Keith, R. Kobayashi, J. Normand, K. Raghavachari, A. P. Rendell, J. C. Burant, S. S. Iyengar, J. Tomasi, M. Cossi, J. M. Millam, M. Klene, C. Adamo, R. Cammi, J. W. Ochterski,

R. L. Martin, K. Morokuma, O. Farkas, J. B. Foresman, D. J. Fox, *Gaussian ~09 Revision C.01*, Gaussian Inc., Wallingford, CT **2010**.
[63] N. M. O'boyle, A. L. Tenderholt, K. M. Langner, *J. Comput. Chem.* **2008**, *29*, 839.
[64] L. Goerigk, S. Grimme, *Phys. Chem. Chem. Phys.* **2011**, *13*, 6670.
[65] N. Mardirossian, M. Head-Gordon, *Mol. Phys.* **2017**, *115*, 2315.
[66] L. Goerigk, A. Hansen, C. Bauer, S. Ehrlich, A. Najibi, S. Grimme, *Phys. Chem. Chem. Phys.* **2017**, *19*, 32184.
[67] R. Pérez-Soto, M. Besora, F. Maseras, *Org. Lett.* **2020**, *22*, 2873.
[68] J. G. Brandenburg, C. Bannwarth, A. Hansen, S. Grimme, *J. Chem. Phys.* **2018**, *148*, 064104.
[69] J. Zheng, *Science* **2006**, *313*, 1951.
[70] J. M. Lehn, *Dynamic Stereochemistry*, Springer, Berlin, Heidelberg **1970**, p. 311.
[71] N. Tanaka, Y. Xiao, A. C. Lasaga, *J. Atmos. Chem.* **1996**, *23*, 37.
[72] J. Burkholder, S. Sander, J. Abbatt, J. Barker, C. Cappa, J. Crounse, T. Dibble, R. Huie, C. Kolb, M. Kurylo, VL Orkin, *Chemical kinetics and photochemical data for use in atmospheric studies; evaluation number, 19*, JPL Publication, Jet Propulsion Laboratory, Pasadena **2020**.
[73] P. Pracht, S. Grimme, *Chem. A Eur. J.* **2021**, *125*, 5681.
[74] R. Krishnan, J. S. Binkley, R. Seeger, J. A. Pople, *J. Chem. Phys.* **1980**, *72*, 650.
[75] Y. Zhao, D. G. Truhlar, *Theor. Chem. Acc.* **2007**, *120*, 215.
[76] R. N. Goldberg, N. Kishore, R. M. Lennen, *J. Phys. Chem. Ref. Data* **2002**, *31*, 231.
[77] P. Neta, P. Maruthamuthu, P. M. Carton, R. W. Fessenden, *J. Phys. Chem.* **1978**, *82*, 1875.
[78] A. J. Kirby, P. W. Lancaster, *J. Chem. Soc., Perkin Trans. 2* **1972**, 1206.
[79] R. Karaman, *Comput. Theor. Chem.* **2011**, *974*, 133.
[80] B. S. Souza, J. R. Mora, E. H. Wanderlind, R. M. Clementin, J. C. Gesser, H. D. Fiedler, F. Nome, F. M. Menger, *Angew. Chem. Int. Ed.* **2017**, *56*, 5345.
[81] S. Su, F.-S. Du, Z.-C. Li, *Org. Biomol. Chem.* **2017**, *15*, 8384.
[82] J.-D. Chai, M. Head-Gordon, *Phys. Chem. Chem. Phys.* **2008**, *10*, 6615.
[83] S. E. Coelho, F. S. S. Schneider, D. C. de Oliveira, G. L. Tripodi, M. N. Eberlin, G. F. Caramori, B. de Souza, J. B. Domingos, *ACS Catal.* **2019**, *9*, 3792.
[84] B. L. Oliveira, B. J. Stenton, V. B. Unnikrishnan, C. R. de Almeida, J. Conde, M. Negrão, F. S. S. Schneider, C. Cordeiro, M. G. Ferreira, G. F. Caramori, J. B. Domingos, R. Fior, G. J. L. Bernardes, *J. Am. Chem. Soc.* **2020**, *142*, 10869.
[85] B. Partopour, A. G. Dixon, *Ind. Eng. Chem. Res.* **2019**, *58*, 5733.

SUPPORTING INFORMATION

Additional supporting information may be found in the online version of the article at the publisher's website.

How to cite this article: F. S. S. Schneider, G. F. Caramori, *J. Comput. Chem.* **2022**, 1. https://doi.org/10.1002/jcc.26861